Experimental preparation of eight-partite cluster state for photonic qumodes

Xiaolong Su, Yaping Zhao, Shuhong Hao, Xiaojun Jia, Changde Xie, and Kunchi Peng*

State Key Laboratory of Quantum Optics and Quantum Optics Devices, Institute of Opto-Electronics, Shanxi University, Taiyuan 030006,China

**Corresponding author: kcpeng@sxu.edu.cn*

Received October 1, 2012; revised November 1, 2012; accepted November 7, 2012; posted November 7, 2012 (Doc. ID 177045); published December 12, 2012

The preparation of multipartite entangled states is the prerequisite for exploring quantum information networks and quantum computation. In this Letter, we present what we believe is the first experimental demonstration of an eight-partite spatially separated continuous variable (CV) cluster state of optical modes. Via the linearly optical transformation of eight squeezed states of light, the eight-partite cluster entangled state with amplitude and phase quadrature correlations are prepared. The generated eight entangled photonic qumodes are spatially separated, which provides valuable quantum resources for implementing CV quantum information protocols. © 2012 Optical Society of America

OCIS codes: 270.6570, 190.4410.

In a one-way quantum computation (QC) model, the quantum bits (qubits) and quantum modes (qumodes) are first initialized in a multipartite cluster entangled state, then a variety of quantum logical operations can be achieved via the single-qubit (qumode) projective measurement and the classical feed forward of the measured outcomes, where the order and choices of measurements are determined by the required algorithm [1–3]. In contrast to the probabilistic generation of photonic qubits in most cases, continuous variable (CV) cluster states of qumodes are produced in an unconditional fashion and thus the one-way QC with CV cluster entangled states of optical modes can be implemented deterministically [4–13].

Following the theoretical proposals on one-way CVQC, the principally experimental demonstrations of various one-way QC logical operations over CVs were achieved using bipartite and four-partite cluster entangled photonic qumodes, respectively [6–9]. To develop a more complicated QC, larger-cluster states with more numbers of entangled qubits (qumodes) are desired. In this Letter, we present what we believe is the first experimental production of a CV eight-partite cluster state for photonic qumodes. The initial resource quantum states are eight quadrature squeezed states of light, which are transformed by a specially designed beam-splitter network to the eight-partite cluster state. The entanglement feature among the obtained eight space-separated photonic qumodes is confirmed by the fully inseparability criteria of CV multipartite entangled states [14].

The CV cluster quadrature correlations (so-called nullifiers) can be expressed by $\hat{p}_a - \sum_{b\in N_a}\hat{x}_b = \delta_a$, $\forall a \in G$ where $\hat{x}_a = (\hat{a} + \hat{a}^\dagger)/2$ and $\hat{p}_a = (\hat{a} - \hat{a}^\dagger)/2i$ stand for quadrature-amplitude and quadrature-phase operators of an optical mode $\hat{a}$, respectively [5,15]. The subscript a (b) expresses the designated mode $\hat{a}$ ($\hat{b}$). The modes of $a \in G$ denote the vertices of the graph G, while the modes of $b \in N_a$ are the nearest neighbors of mode $\hat{a}$. δ_a express the excess noises resulting from the imperfect quantum correlations. For an ideal cluster state, the nullifiers trend to zero, which stands for a simultaneous zero eigenstate of the quadrature combination [5].

Figure 1(a) shows the graph representation of a CV eight-partite linear cluster state. Each node corresponds to an optical mode and the connection lines between neighboring nodes stand for the interaction between the connected two nodes. The scheme of generating CV multipartite entangled states commonly used in experiments are to achieve a linearly optical transformation of input squeezed states on a specific beam-splitter network [16]. Assuming $\hat{a}_l$ and U_{kl} stand for the input squeezed state and the unitary matrix of a given beam-splitter network, respectively, the output optical modes after the transformation are given by $\hat{b}_k = \sum_l U_{kl}\hat{a}_l$, where the subscripts l and k express the designated input and output modes, respectively. In our experiment, four quadrature-amplitude $\hat{x}$-squeezed states, $\hat{a}_m = e^{-r}\hat{x}_m^{(0)} + ie^{+r}\hat{p}_m^{(0)}(m = 1,3,5,7)$, and four quadrature-phase $\hat{p}$-squeezed states, $\hat{a}_n = e^{+r}\hat{x}_n^{(0)} + ie^{-r}\hat{p}_n^{(0)}(n = 2,4,6,8)$, are applied, where

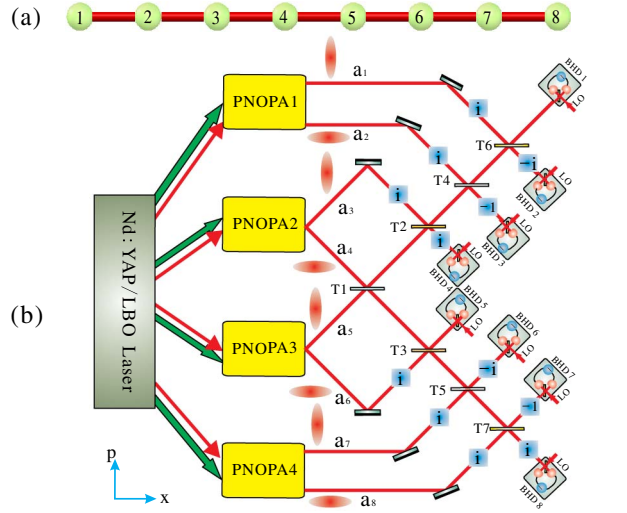

Fig. 1. (Color online) (a) Graph representation of the eight-partite linear cluster state. (b) Schematic of experimental setup for preparing a CV eight-partite cluster state. T: transmission efficient of beam splitter, Boxes including i are Fourier transforms, $-i$ is a $-90°$ rotation, and -1 is a $180°$ rotation. BHD, balanced homodyne detector; and LO, local oscillator.

$\hat{x}_j^{(0)}$ and $\hat{p}_j^{(0)}$ denote the quadrature-amplitude and the quadrature-phase operators of the corresponding vacuum field, respectively. In this case, r is the squeezing parameter, $r = 0$, and $r = +\infty$ correspond to no squeezing and the ideally perfect squeezing, respectively. The unitary matrix U_L for generating the CV eight-partite linear cluster state deduced with the method given in [16] is

$$\begin{pmatrix} \frac{i}{\sqrt{2}} & \frac{i}{\sqrt{3}} & \frac{i}{\sqrt{10}} & \frac{\sqrt{3}}{\sqrt{170}} & \frac{\sqrt{5}}{\sqrt{102}} & 0 & 0 & 0 \\ \frac{-1}{\sqrt{2}} & \frac{1}{\sqrt{3}} & \frac{1}{\sqrt{10}} & \frac{-i\sqrt{3}}{\sqrt{170}} & \frac{-i\sqrt{5}}{\sqrt{102}} & 0 & 0 & 0 \\ 0 & \frac{i}{\sqrt{3}} & \frac{-i\sqrt{2}}{\sqrt{5}} & \frac{-\sqrt{6}}{\sqrt{85}} & \frac{-\sqrt{10}}{\sqrt{51}} & 0 & 0 & 0 \\ 0 & 0 & \frac{\sqrt{2}}{\sqrt{5}} & \frac{3i\sqrt{3}}{\sqrt{170}} & \frac{i\sqrt{15}}{\sqrt{34}} & 0 & 0 & 0 \\ 0 & 0 & 0 & \frac{\sqrt{15}}{\sqrt{34}} & \frac{-3\sqrt{3}}{\sqrt{170}} & \frac{i\sqrt{2}}{\sqrt{5}} & 0 & 0 \\ 0 & 0 & 0 & \frac{i\sqrt{10}}{\sqrt{51}} & \frac{-i\sqrt{6}}{\sqrt{85}} & \frac{\sqrt{2}}{\sqrt{5}} & \frac{1}{\sqrt{3}} & 0 \\ 0 & 0 & 0 & \frac{-\sqrt{5}}{\sqrt{102}} & \frac{\sqrt{3}}{\sqrt{170}} & \frac{i}{\sqrt{10}} & \frac{-i}{\sqrt{3}} & \frac{-i}{\sqrt{2}} \\ 0 & 0 & 0 & \frac{-i\sqrt{5}}{\sqrt{102}} & \frac{i\sqrt{3}}{\sqrt{170}} & \frac{-1}{\sqrt{10}} & \frac{1}{\sqrt{3}} & \frac{-1}{\sqrt{2}} \end{pmatrix}. \quad (1)$$

The unitary matrix can be decomposed into a beam-splitter network consisting of seven beam-splitters $U_L = F_8 I_7(-1) F_6^{\dagger} F_4 I_3(-1) F_2^{\dagger} B_{78}^{-}(1/2) F_8 B_{12}^{-}(1/2) F_1 B_{67}^{-}(1/3) F_7 B_{23}^{-}(1/3) F_2 B_{56}^{-}(2/5) F_6 B_{34}^{-}(2/5) F_3 B_{45}^{+}(25/34)$, where F_k denotes the Fourier transformation of mode k, which corresponds to a 90° rotation in phase space; $B_{kl}^{\pm}(T_j)$ stands for the linearly optical transformation on the jth beam-splitter with the transmission of T_j $(j = 1, 2, 3 \ldots 7)$, where $(B_{kl}^{\pm})_{kk} = \sqrt{1-T}$, $(B_{kl}^{\pm})_{kl} = \sqrt{T}$, $(B_{kl}^{\pm})_{lk} = \pm\sqrt{T}$, and $(B_{kl}^{\pm})_{ll} = \mp\sqrt{1-T}$, are elements of beam-splitter matrix. $I_k(-1) = e^{i\pi}$ corresponds to a 180° rotation in phase space.

Figure 1(b) shows the schematic of the experimental set-up for preparing the CV eight-partite linear cluster state. The four $\hat{x}$-squeezed and four $\hat{p}$-squeezed states are produced by four polarization nondegenerate optical parametric amplifiers (PNOPAs) pumped by a common laser source, which is a CW intracavity frequency-doubled and frequency-stabilized Nd:YAP/LBO (Nd-doped $YAlO_3$ perorskite/lithium triborate) [17]. The output fundamental wave at 1080 nm wavelength is used for the injected signals of PNOPAs and the local oscillators of the balanced homodyne detectors (BHDs). The second-harmonic wave at 540 nm wavelength serves as the pump field of the four PNOPAs, through which an intracavity frequency-down-conversion process a pair of signal and idler modes with the identical frequency at 1080 nm and the orthogonal polarizations are generated [18]. Each of PNOPAs consists of an α-cut type-II KTP crystal and a concave mirror [18]. The front face of the KTP was coated to be used for the input coupler and the concave mirror, which served as the output coupler of the squeezed states, is mounted on a piezo-electric transducer for locking actively the cavity length of PNOPA on resonance with the injected signal at 1080 nm. The transmissions of the input coupler at 540 and 1080 nm are 99.8% and 0.04%, respectively. The transmissions of the output coupler at 540 and 1080 nm are 0.5% and 5.2%, respectively. The finesses of the PNOPA for 540 and 1080 nm are 3 and 117, respectively. In our experiment, the four PNOPAs are operated at the parametric deamplification situation, [i.e., the phase difference between the pump field and the injected signal is $(2n+1)\pi$ (n is an integer)]. Under this condition, the coupled modes at +45° and −45° polarization directions are the quadrature-amplitude and the quadrature-phase squeezed states, respectively [10,19].

When the transmissions of the seven beam-splitters are chosen as $T_1 = 25/34$, $T_2 = T_3 = 2/5$, $T_4 = T_5 = 1/3$, $T_6 = T_7 = 1/2$, the eight output optical modes are in a eight-partite CV linear cluster state. For our experimental system all four PNOPAs have the identical configuration and are operated under the same conditions. So, the eight initial squeezed states own the same squeezed parameter r. In this case, the excess noises of the nullifiers for the eight-partite linear CV cluster state are $\delta_1 = \sqrt{2}e^{-r}\hat{x}_1^{(0)}$, $\delta_2 = \sqrt{3}e^{-r}\hat{p}_2^{(0)}$, $\delta_3 = \frac{1}{\sqrt{2}}e^{-r}\hat{x}_1^{(0)} - \sqrt{\frac{5}{2}}e^{-r}\hat{x}_3^{(0)}$, $\delta_4 = \frac{1}{\sqrt{3}}e^{-r}\hat{p}_2^{(0)} + \sqrt{\frac{2}{5}}e^{-r}\hat{p}_6^{(0)} + \sqrt{\frac{34}{15}}e^{-r}\hat{x}_5^{(0)}$, $\delta_5 = \sqrt{\frac{34}{15}}e^{-r}\hat{p}_4^{(0)} - \sqrt{\frac{2}{5}}e^{-r}\hat{x}_3^{(0)} - \frac{1}{\sqrt{3}}e^{-r}\hat{x}_7^{(0)}$, $\delta_6 = \sqrt{\frac{5}{2}}e^{-r}\hat{p}_6^{(0)} - \frac{1}{\sqrt{2}}e^{-r}\hat{p}_8^{(0)}$, $\delta_7 = -\sqrt{3}e^{-r}\hat{x}_7^{(0)}$ and $\delta_8 = -\sqrt{2}e^{-r}\hat{p}_8^{(0)}$, respectively.

According to the inseparability criteria for CV multipartite entangled states proposed by van Loock and Furusawa [14], we deduced the inseparability criteria for the CV eight-partite linear cluster state, which are

$$V(\hat{p}_1 - \hat{x}_2) + V(\hat{p}_2 - \hat{x}_1 - \hat{x}_3) < 1, \quad (2a)$$

$$V(\hat{p}_2 - \hat{x}_1 - \hat{x}_3) + V(\hat{p}_3 - \hat{x}_2 - \hat{x}_4) < 1, \quad (2b)$$

$$V(\hat{p}_3 - \hat{x}_2 - \hat{x}_4) + V(\hat{p}_4 - \hat{x}_3 - \hat{x}_5) < 1, \quad (2c)$$

$$V(\hat{p}_4 - \hat{x}_3 - \hat{x}_5) + V(\hat{p}_5 - \hat{x}_4 - \hat{x}_6) < 1, \quad (2d)$$

$$V(\hat{p}_5 - \hat{x}_4 - \hat{x}_6) + V(\hat{p}_6 - \hat{x}_5 - \hat{x}_7) < 1, \quad (2e)$$

$$V(\hat{p}_6 - \hat{x}_5 - \hat{x}_7) + V(\hat{p}_7 - \hat{x}_6 - \hat{x}_8) < 1, \quad (2f)$$

$$V(\hat{p}_7 - \hat{x}_6 - \hat{x}_8) + V(\hat{p}_8 - \hat{x}_7) < 1, \quad (2g)$$

where the left-hand sides and right-hand sides of these inequalities are the combination of variances of nullifiers and the normalized boundary, respectively. When all variance combinations at left-hand sides are smaller than 1, the eight qumodes are in an eight-partite cluster state.

The experimentally measured initial squeezing degrees of the output fields from four PNOPAs are 4.30 ± 0.07 dB below the quantum noise level, which corresponds to the squeezing parameter $r = 0.50 \pm 0.02$. For our system, the total transmission efficiency of squeezed beams are about 87% and the detection efficiency is about 90%, which lead to the efficient squeezing parameter is $r_e = 0.30$. During the measurements, the pump power

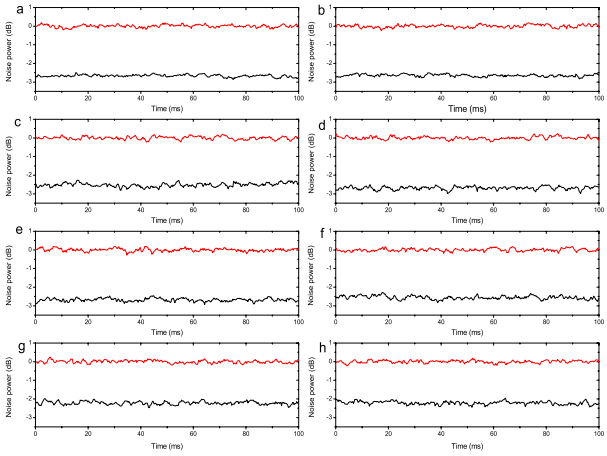

Fig. 2. (Color online) Measured noise powers of an eight-partite linear cluster state. The upper and lower curves in all graphs are the normalized quantum noise level and correlation variances of nullifiers, respectively. (a–h) are noise powers of $V(\hat{p}_1 - \hat{x}_2)$, $V(\hat{p}_2 - \hat{x}_1 - \hat{x}_3)$, $V(\hat{p}_3 - \hat{x}_2 - \hat{x}_4)$, $V(\hat{p}_4 - \hat{x}_3 - \hat{x}_5)$, $V(\hat{p}_5 - \hat{x}_4 - \hat{x}_6)$, $V(\hat{p}_6 - \hat{x}_5 - \hat{x}_7)$, $V(\hat{p}_7 - \hat{x}_6 - \hat{x}_8)$, and $V(\hat{p}_8 - \hat{x}_7)$, respectively. The measurement frequency is 2 MHz, the resolution bandwidth is 30 kHz, and the video bandwidth is 100 Hz.

of PNOPAs at 540 nm wavelength is kept at ~180 mW, which is below the oscillation threshold of 240 mW, and the intensity of the injected signal at 1080 nm is 10 mW. The phase difference on of the each beam-splitters is locked according to the above-mentioned requirements. The light intensity of the local oscillator in all BHDs is set to ~5 mW.

The correlation variances measured experimentally are shown in Fig. 2. They are $V(\hat{p}_1 - \hat{x}_2) = -2.67 \pm 0.06$ dB, $V(\hat{p}_2 - \hat{x}_1 - \hat{x}_3) = -2.65 \pm 0.13$ dB, $V(\hat{p}_3 - \hat{x}_2 - \hat{x}_4) = -2.52 \pm 0.20$ dB, $V(\hat{p}_4 - \hat{x}_3 - \hat{x}_5) = -2.69 \pm 0.09$ dB, $V(\hat{p}_5 - \hat{x}_4 - \hat{x}_6) = -2.68 \pm 0.08$ dB, $V(\hat{p}_6 - \hat{x}_5 - \hat{x}_7) = -2.56 \pm 0.10$ dB, $V(\hat{p}_7 - \hat{x}_6 - \hat{x}_8) = -2.22 \pm 0.09$ dB, and $V(\hat{p}_8 - \hat{x}_7) = -2.21 \pm 0.09$ dB. From these measured results we can calculate the combinations of the correlation variances in the left-hand sides of the inequalities (2a)–(2g), which are 0.68 ± 0.02, 0.83 ± 0.02, 0.82 ± 0.02, 0.81 ± 0.02, 0.82 ± 0.02, 0.87 ± 0.02, and 0.75 ± 0.02, respectively. Since all of these values are smaller than the boundary, the prepared eight photonic qumodes satisfy the inseparability criteria and form an eight-partite cluster entangled state.

In conclusion, the eight-partite cluster state of optical qumodes provide the necessary resources for implementing a more complex one-way CVQC. Recently, a novel hybrid quantum information processing (QIP) protocol, which combines the advantages of both optical qubits and qumodes, has been theoretically proposed [20]. The hybrid system will offer a better QIP capacity with unitary fidelity and high success rate [21]. For practical applications, the high-performance quantum optical devices ideally integrated on a single optical chip should be developed. The recent improvements in the fabrication of optoelectronics and integrated optics open a door to the prospect of optical on-chip QIP.

This research was supported by the Shanxi Scholarship Council of China (Grant No. 2012-010), the National Basic Research Program of China (Grant No. 2010CB923103), and the NSFC (Grant Nos. 11174188, 61121064).

References

1. R. Raussendorf and H. J. Briegel, Phys. Rev. Lett. **86**, 5188 (2001).
2. N. C. Menicucci, P. van Loock, M. Gu, C. Weedbrook, T. C. Ralph, and M. A. Nielsen, Phys. Rev. Lett. **97**, 110501 (2006).
3. C. Weedbrook, S. Pirandola, R. García-Patrón, N. J. Cerf, T. C. Ralph, J. H. Shapiro, and S. Lloyd, Rev. Mod. Phys. **84**, 621 (2012).
4. P. van Loock, J. Opt. Soc. Am. B **24**, 340 (2007).
5. M. Gu, C. Weedbrook, N. C. Menicucci, T. C. Ralph, and P. van Loock, Phys. Rev. A **79**, 062318 (2009).
6. Y. Miwa, J. I. Yoshikawa, P. van Loock, and A. Furusawa, Phys. Rev. A **80**, 050303(R) (2009).
7. Y. Wang, X. Su, H. Shen, A. Tan, C. Xie, and K. Peng, Phys. Rev. A **81**, 022311 (2010).
8. R. Ukai, N. Iwata, Y. Shimokawa, S. C. Armstrong, A. Politi, J. Yoshikawa, P. van Loock, and A. Furusawa, Phys. Rev. Lett. **106**, 240504 (2011).
9. R. Ukai, S. Yokoyama, J. I. Yoshikawa, P. van Loock, and A. Furusawa, Phys. Rev. Lett. **107**, 250501 (2011).
10. X. Su, A. Tan, X. Jia, J. Zhang, C. Xie, and K. Peng, Phys. Rev. Lett. **98**, 070502 (2007).
11. M. Yukawa, R. Ukai, P. van Loock, and A. Furusawa, Phys. Rev. A **78**, 012301 (2008).
12. A. Tan, Y. Wang, X. Jin, X. Su, X. Jia, J. Zhang, C. Xie, and K. Peng, Phys. Rev. A **78**, 013828 (2008).
13. M. Pysher, Y. Miwa, R. Shahrokhshahi, R. Bloomer, and O. Pfister, Phys. Rev. Lett. **107**, 030505 (2011).
14. P. van Loock and A. Furusawa, Phys. Rev. A **67**, 052315 (2003).
15. J. Zhang and S. L. Braunstein, Phys. Rev. A **73**, 032318 (2006).
16. P. van Loock, C. Weedbrook, and M. Gu, Phys. Rev. A **76**, 032321 (2007).
17. Y. Wang, Y. Zheng, C. Xie, and K. Peng, IEEE J. Quantum Electron. **47**, 1006 (2011).
18. Y. Wang, H. Shen, X. Jin, X. Su, C. Xie, and K. Peng, Opt. Express **18**, 6149 (2010).
19. Y. Zhang, H. Wang, X. Li, J. Jing, C. Xie, and K. Peng, Phys. Rev. A **62**, 023813 (2000).
20. P. van Loock, Laser Photon. Rev. **5**, 167 (2011).
21. J. L. O'Brien, A. Furusawa, and J. Vučković, Nat. Photonics **3**, 687 (2009).